Molecular Crystals and Liquid Crystals
Publication details, including instructions for authors and subscription information:
http://www.tandfonline.com/loi/gmcl16

^{57}Fe Mossbauer Study of Four Ferroene Derivatives in a Smectic B Liquid Crystalline Glass

V. O. Aimiuwu [a] & D. L. Uhrich [a]
[a] Department of Physics and Liquid Crystal, Institute, Kent State University, Kent, Ohio, 44242
Version of record first published: 28 Mar 2007.

To cite this article: V. O. Aimiuwu & D. L. Uhrich (1977): ^{57}Fe Mossbauer Study of Four Ferroene Derivatives in a Smectic B Liquid Crystalline Glass, Molecular Crystals and Liquid Crystals, 43:3-4, 295-312

To link to this article: http://dx.doi.org/10.1080/00268947708084676

Mol. Cryst., Liq. Cryst., 1977, Vol.43, pp. 295–312

Printed in Holland

^{57}Fe Mossbauer Study of Four Ferrocene Derivatives in a Smectic B Liquid Crystalline Glass†

V. O. AIMIUWU and D. L. UHRICH

Department of Physics and Liquid Crystal Institute, Kent State University, Kent, Ohio 44242

(*Received April 7, 1977*)

Two monosubstituted ferrocenes [ferrocenyl-4′-methoxyaniline (FMA) and ferrocenyl-4′-*n*-butylaniline (FBA)] and two disubstituted ferrocenes [1-1′-di-*n*-octanoyl ferrocene (DOF) and dibenzyl 1,1′-ferrocene dicarboxylate (DFD)] were introduced into the smectic B liquid crystalline phase of 4-*n*-butoxybenzylidene-4′-*n*-octylaniline (BBOA, or 40.8). The resulting systems (3 solutions and one suspension) were studied by ^{57}Fe Mossbauer spectroscopy in the smectic B glass of BBOA at 77°K. The recoil-free fraction, f, and the line asymmetry of the quadrupole split doublet (given by the area ratio of the π and the σ transitions A_π/A_σ) were observed as functions of the angle θ between the gamma ray direction and the preferred molecular direction as determined by a 9 kG external magnetic field.

Analysis of the A_π/A_σ versus θ measurements for solutions of DOF, FBA, and FMA in BBOA confirms a positive electric field gradient (V_{zz}) normal to the cyclopentadienyl rings and yields an intra-molecular vibrational anisotropy $\varepsilon_M = 0$ for DOF and $\varepsilon_M = 0.20$ for FBA and FMA. The area ratio measurements also give the solute order parameter S as follows: 0.11 for 1.5% and 2.0% DOF in BBOA; 0.27 for 1.0% FBA in BBOA; and 0.37 for 1.0% FMA in BBOA. These S values for the solutes are explained in terms of molecular structure and shapes of the solute and the host BBOA molecules. The f versus θ measurements give the lattice contribution (ε_L) to the nuclear vibrational ellipsoid. The values obtained for ε_L are 0.04 (FMA); 0.07 (DOF); and 0.12 (FMA). These values are discussed with respect to the shapes and locations of the solute molecules relative to the central-core and end-chain regions of the BBOA molecules. Further, these results are compared to previously reported values for Sn-bearing molecules.

I INTRODUCTION

Investigations of liquid crystalline phases by using Mossbauer probe molecules as solutes have recently been reported.[1–10] Emphasis was placed on the ordering ability and structure of the mesophases as well as the intramolecular vibrations of the Mossbauer nuclei. Of the three Mossbauer

† Presented at the Sixth International Conference on Liquid Crystals, Kent State University, Kent, Ohio 44242. August, 1976.

This work was supported in part by the National Science Foundation, under Grant Nos. GH 34164X and DMR 7411373.

isotopes that have been used in these investigations, the coordination chemistry of ^{129}I and ^{119}Sn ensures the availability of long molecules with rather rigid central-core regions which give them structural properties similar to the liquid crystal molecules, themselves. Consequently, ^{129}I and ^{119}Sn bearing molecules are more soluble in liquid crystals than presently available ^{57}Fe bearing molecules which lack the above structural characteristics. For the latter, long and linear molecules are approximated by ferrocene derivatives which are less soluble. In particular, homogeneous solutions of several ferrocene derivatives in the liquid crystal, 4-*n*-butoxybenzylidene-4′-*n*-octylaniline (BBOA or 40.8) could not be obtained for solute concentrations greater than 2% by weight. In contrast, solutions of 7% for triethyltin palmitate[3] and 20% for 4-*n*-hexoybenzylidene-4′-^{129}iodaniline[9] in 4-*n*-hexoxybenzylidene-4′-*n*-propylaniline (HOAB or 60.3) have been reported.

Extensive work has been carried out with Sn-bearing solutes, where the Wilson–Uhrich theory has successfully accounted for the observed angular dependence of the Mossbauer parameters.[2–4,7,10] This theory, however, fails to account for experimental observations for Fe-bearing solutes.[6] The difference between the symmetry of the two sets of molecules was probably responsible for this discrepancy. Consequently, while the main component of the electric field gradient (efg) tensor, V_{zz}, was colinear with the long molecular axis for the case of the Sn-bearing solutes used, it is approximately perpendicular to the long molecular axis for the ferrocene derivatives. (See Figure 1.) In this paper, the Wilson–Uhrich theory is extended to the situation where V_{zz} makes any angle β with the long molecular axis. Furthermore, we have introduced four ferrocene derivatives into BBOA and the theory is shown to adequately account for the orientation dependence of both the area ratio (A_π/A_σ) of the quadrupole split doublet and the total intensity (f) of the Mossbauer solution spectra. The area ratio (A_π/A_σ) is for the quadrupole doublet resulting from the hyperfine interaction of the quadrupole moment of the first excited state (of Fe^{57} or Sn^{119}) and the efg at the nuclear site. Here, π denotes the $|\frac{3}{2}, \pm\frac{3}{2}\rangle \rightarrow |\frac{1}{2}, \pm\frac{1}{2}\rangle$ transition and σ denotes the $|\frac{3}{2}, \pm\frac{1}{2}\rangle \rightarrow |\frac{1}{2}, \pm\frac{1}{2}\rangle$ transition. Measurements of A_π/A_σ and f were obtained as the function of the angle θ between the preferred molecular direction (as

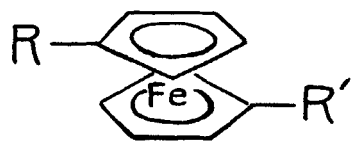

FIGURE 1 Approximate shape of a disubstituted ferrocene derivative. Here R and R' represent the tails which are attached to the cyclopentadienal rings. For a monosubstituted ferrocene derivative one of the tails would be replaced by a hydrogen atom.

determined by an external magnetic field) and the Mossbauer γ-beam direction. All the measurements were performed at $\sim 77°K$ in the smectic B glass phase of BBOA.

The theory, experimental procedures, liquid crystal properties and solution integrity, and the application of the theory to the experimental results for the ferrocene derivatives in BBOA will be presented in the following sections.

II THEORY

Let us consider a long molecule which is not necessarily axially symmetric about its long axis (c). For a homogeneous solution of this compound in a liquid crystal the long molecular axes of the solute molecules will be aligned by a magnetic field, H, in the nematic liquid crystalline phase.[3, 11, 12] In such a system, the distribution of the long molecular axes about H is given by Saupe's angular distribution function:[12]

$$D = Ce^{-(q/KT)\sin^2\delta} \tag{1}$$

where q is an interaction energy, T is the absolute temperature, K is Boltzmann's constant and δ is the angle between c and H. If the nematic phase is cooled to a higher order smectic phase in the presence of H and subsequently frozen into a smectic glass, the molecular alignment is preserved and the distribution function (Eq. 1) becomes time independent and represents the spatial distribution of the molecular axes about the preferred direction. Figure 2a illustrates the relationship between the laboratory (or magnetic field) system (x, y, z) and the molecular system (a, b, c). A unique orthogonal

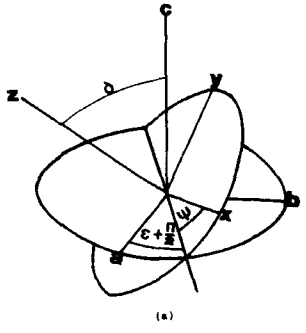

FIGURE 2(a) Illustration of the relation between the laboratory system (x, y, z) and the molecular system (a, b, c). Here $(\varepsilon + \pi/2, \delta, \psi)$ are the Euler angles.

matrix A rotates the latter into the former:[13]

$$A(\varepsilon, \delta, \psi) = \begin{pmatrix} -\cos\psi & \sin\varepsilon - \cos\delta & \cos\varepsilon & \sin\psi & & \\ \sin\psi & \sin\varepsilon - \cos\delta & \cos\varepsilon & \cos\psi & & \\ \sin\delta & \cos\varepsilon & & & & \\ & \cos\psi & \cos\varepsilon - \cos\delta & \sin\varepsilon & \sin\psi & \sin\psi & \sin\delta \\ & -\sin\psi & \cos\varepsilon - \cos\delta & \sin\varepsilon & \cos\psi & \cos\psi & \sin\delta \\ & \sin\delta & \sin\varepsilon & & & \cos\delta & \end{pmatrix} \tag{2}$$

where $(\varepsilon + \pi/2, \delta, \psi)$ are Euler angles.[14]

The next step is to use this matrix to find appropriate expressions for f and A_π/A_σ.

For solute molecules in liquid crystalline glasses, the intramolecular and intermolecular (lattice) vibrations may be considered to be uncoupled as is usually done for molecular crystals.[15] Then $f = f_M f_L$, where f_M and f_L represent the respective contributions of the molecule and the lattice to the recoil-free fraction. It can easily be shown that for a smectic liquid crystalline lattice,[3]

$$f_L \propto \int_0^{2\pi} \exp[-\varepsilon_L(\sin\tau \sin\theta \cos\mu + \cos\theta \cos\tau)^2]\mathrm{d}\mu \tag{3}$$

where θ is the experimentally measurable angle between H and the γ-ray direction (Figure 2b); τ and μ are, respectively, the polar and azimuthal angles of the planar normal in the laboratory system. [τ is commonly referred to as the tilt angle between the preferred molecular direction and the normal to

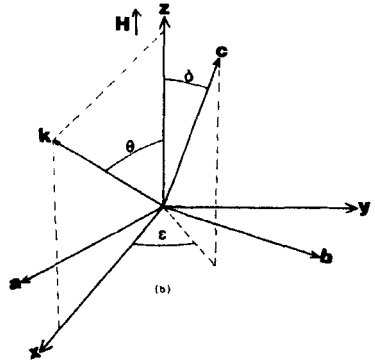

FIGURE 2(b) The laboratory system (x, y, z) is defined so that the magnetic field (H) is parallel to z and so that the gamma ray direction (k) is in the x–z plane. θ is the experimental angle. δ and ε are the polar and azimuthal angles of a given molecule's long molecular axis (c) in the laboratory system.

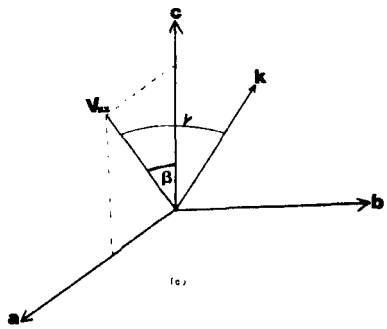

FIGURE 2(c) The gamma direction (k) and the principal axis of the efg (V_{zz}) are shown in the coordinate system of a given molecule. For the ferrocene derivatives $\beta \approx \pi/2$.

the smectic layers.] Since only the molecular preferred direction is determined by H, an average over μ must be performed.

$$\varepsilon_L = k^2(\langle x_{\parallel}^2\rangle_L - \langle x_{\perp}^2\rangle_L) \tag{4}$$

is the lattice contribution to the nuclear vibrational ellipsoid, $\langle x_{\parallel}^2\rangle_L$ and $\langle x_{\perp}^2\rangle_L$ are the mean square displacements, respectively, parallel and perpendicular to the normal of the smectic planes, and k is the magnitude of the wave vector of the Mossbauer γ-ray. For an individual molecule

$$f_M \propto e^{-\varepsilon_M \cos^2\gamma} \tag{5}$$

where γ is the angle $\hat{V}_{zz}$ makes with $\hat{k}$, ε_M is the molecular contribution to the vibrational anisotropy and is defined in a manner similar to ε_L, but with respect to the $\hat{V}_{zz}$ direction. Without any loss of generality, $\hat{V}_{zz}$ can be drawn in the a-c plane of the molecular axis system (See Figure 2c) and $\hat{k}$ in the x-z plane of the laboratory system (See Figure 2b). The matrix A can then be used to express $\cos\gamma$ in terms of $\varepsilon, \delta, \psi, \theta$, and β since $\cos\gamma = \hat{k}\cdot\hat{V}_{zz}$ where $\hat{V}_{zz} = \begin{pmatrix}\sin\beta\\0\\\cos\beta\end{pmatrix}$ and $\hat{k} = A\hat{k}_L$ where $\hat{k}_L = \begin{pmatrix}\sin\theta\\0\\\cos\theta\end{pmatrix}$. Here $\hat{k}$ and $\hat{k}_L$ are represented in the molecular and laboratory frames, respectively. The result is:

$$\begin{aligned}\cos\gamma = {} & (\sin\psi\sin\delta\cos\theta - \cos\psi\sin\varepsilon\sin\theta \\ & - \cos\delta\cos\varepsilon\sin\psi\sin\theta)\sin\beta \\ & + (\sin\delta\cos\varepsilon\sin\theta + \cos\delta\cos\theta)\cos\beta\end{aligned} \tag{6}$$

For a particular θ, γ depends on ε, δ, ψ, and β. All values of ε are possible since the molecular azimuths are uniformly distributed around the field direction. Therefore, one needs to average ε over 2π. The δ dependence must be weighted with Saupe's distribution function and averaged over $\pi/2$ (Eq. 1). Since there is no preference of molecular orientation about c, the a and b axes

of the molecules are considered to be uniformly distributed about their long axes before freezing to the glass phase. All values of ψ are therefore possible and its dependence should be averaged over 2π. Since molecules are not perfectly rigid structures, one would expect that there will be a distribution of β's in the glass phase. Intramolecular bending motions in the normal liquid crystal phases will result in a time average of β about some preferred angle between the long molecular axis and the V_{zz} direction. Upon freezing to the glassy liquid crystal, a spatial distribution of β's about some preferred angle is the result. Consequently, β must be averaged over $\pi/2$ according to a distribution function $f(\beta)$ which is determined by the location of the Mossbauer probe nucleus in the molecule, the flexibility of the intramolecular bonds, and the steric restrictions caused by the molecular packing in the liquid crystalline glass. The final expression for f_M is given by:

$$f_M(\theta) \propto \int_0^{2\pi} d\psi \int_0^{2\pi} d\varepsilon \int_0^{\pi/2} d\beta \int_0^{\pi/2} d\delta\, e^{-\varepsilon_M \cos^2\gamma - (q/KT)\sin^2\delta} \sin\delta f(\beta)\sin\beta \tag{7}$$

where $\cos\gamma$ is given by Eq. 6. Similarly, in the case of an axially symmetric efg, the area ratio becomes:

$$\frac{A_\pi}{A_\sigma}(\theta) = \frac{\int_0^{2\pi} d\psi \int_0^{2\pi} d\varepsilon \int_0^{\pi/2} d\beta \int_0^{\pi/2} d\delta(1 + \cos^2\gamma)e^{-\varepsilon_M \cos^2\gamma - (q/KT)\sin^2\delta}\sin\delta f(\beta)\sin\beta}{\int_0^{2\pi} d\psi \int_0^{2\pi} d\varepsilon \int_0^{\pi/2} d\beta \int_0^{\pi/2} d\delta(\tfrac{5}{3} - \cos^2\gamma)e^{-\varepsilon_M \cos^2\gamma - (q/KT)\sin^2\delta} \sin\delta f(\beta)\sin\beta} \tag{8}$$

By fitting Eq. 8 and the product of Eqs. 3 and 7 to the appropriate experimental measurements, one can, in principle, obtain τ, ε_M, ε_L and q/KT if $f(\beta)$ is known. Then q/KT can be used to evaluate the spatial order parameter, S:

$$S = \frac{\int_0^{\pi/2} \frac{1}{2}(3\cos^2\delta - 1)e^{-(q/KT)\sin^2\delta} \sin\delta\, d\delta}{\int_0^{\pi/2} e^{-(q/KT)\sin^2\delta} \sin\delta\, d\delta} \tag{9}$$

III EXPERIMENTAL

The details of the constant-acceleration Mossbauer spectrometer based on an electromechanical feedback system have been reported elsewhere.[16,17] A Hewlett-Packard 5401 A multichannel analyzer was used to process and store the data. The 30 mc Co-57 source (on a Cu matrix) was purchased from the New England Nuclear Corp. Both powdered sodium nitroprusside and

NBS α-Fe (SRM No. 1541) standard absorbers were used to calibrate the system.

The liquid crystalline solvent was BBOA.[18] It possesses three liquid crystalline phases which are listed below with the transition temperatures:

$$\text{Crystal} \xrightarrow{30\ C} \text{Smectic B} \underset{}{\overset{48\ C}{\rightleftharpoons}} \text{Smectic A} \underset{}{\overset{63\ C}{\rightleftharpoons}} \text{Nematic} \underset{}{\overset{79\ C}{\rightleftharpoons}} \text{isotropic liquid}$$

The smectic B phase of BBOA belongs to the B_1 classification of deVries[19] and is also called the "ordinary B." It is optically uniaxial, with the preferred direction of the molecular long axes perpendicular to the smectic plane ($\tau = 0$) within which the molecules arrange themselves in a two-dimensional lattice.

The four ferrocene derivatives used in this study are presented in Table I, together with the percent concentrations (by weight) which were used. The samples were made by dissolving weighed amounts of the solutes in BBOA, by heating to the isotropic phase in vacuo, The integrity of the samples was checked by x-ray and differential thermal analysis (DTA). In particular, room temperature x-ray pictures on the Mossbauer samples were checked for the presence of an undissolved solid component. Furthermore, room temperature Mossbauer runs in the supercooled smectic B phase were used to distinguish between true solutions and suspensions of microcrystallites. If the Mossbauer absorption was evident immediately after cooling to room temperature then either the ferrocene derivative had formed a suspension of microcrystallites or the BBOA had crystallized, or both. If no effect was evident the integrity of the solution was maintained, or if crystallites had formed they were too small to give a non-vanishing f-factor. The x-ray analysis and the Mossbauer technique were used in conjunction to determine if a solution was formed. The latter was the easier and indicated gross

TABLE I

Solute	Chemical name	Concentration (weight %)
$C_5H_5FeC_5H_4CHN(C_6H_4))OCH_3$	Ferrocynal-4'-methoxyaniline (FMA)	1, 2
$C_5H_5FeC_5H_4CHN(C_6H_4)(CH_2)_3CH_3$	Ferrocynal-4'-butylaniline (FBA)	1
$Fe[C_5H_4COOCH_2(C_6H_5)]_2$	Dibenzyl 1-1' Ferrocene dicarboxylate (DFD)	1, 2
$Fe[C_5H_4COC_7H_{15}]_2$	1,1'Di-*n*-octanoyl ferrocene (DOF)	1.5, 2, 3

deviation from true solutions and the former was used to check all the samples which were apparent solutions according to the Mossbauer runs.

The alignment procedure consisted of cooling the sample from the isotropic liquid (~85°C) through the smectic A, and smectic B phases to room temperature in the presence of a 9 kG magnetic field. The disk-shaped sample was then removed from the field and attached to the cold finger tail of an Austin Science Associates' Dewar (Assad-77) capable of maintaining the sample at a fixed temperature. The cold bath used was liquid Nitrogen (77–78°K) and the Mossbauer gamma beam was in all cases directed normal to the disk face.

The spectrum of each run was fitted with a two component Lorentzian using a Burroughs 5500 computer, whose output yielded the area ratio, the linewidth Γ and the percent effect of the absorption p. The recoil-free intensity was taken as proportional to the sum of the products of the last two, that is, $f = \sum(\pi/2)p\Gamma$.

For each sample several (three or more) measurements were taken at seven equally-spaced orientations for $0° \leq \theta \leq 90°$. The average values for the Mossbauer parameters at each of these orientations were taken as the experimental data points. The mean of the standard deviations at the seven orientations was taken as the standard deviation (σ) of the experimental points. The σ values are shown as the error bars in the A_π/A_σ vs. θ and f vs. θ plots (vide infra).

IV EXPERIMENTAL RESULTS AND DISCUSSION

Mossbauer runs on both 3% DOF and 2% FMA in BBOA at 77°K showed that A_π/A_σ tended to one and f increased with run time. Thus, the DOF and FMA were coming out of solution in these samples. In addition, room temperature Mossbauer runs on 2% DFD in BBOA yielded a non-zero intensity showing that the DFD molecules were coming out of solution. Consequently solutions of lower concentration of DFD, DOF, and FMA were prepared. Room temperature x-ray analysis confirmed homogeneous solutions for 1% FMA, 1% FBA, 1.5% DOF and 2% DOF in BBOA. Conversely, it also showed the sample of 1% DFD in BBOA had formed a uniform suspension of minute crystallites of the solute. These crystallites were quite small, however, because the room temperature supercooled smectic B phase yielded no Mossbauer effect for this sample.

For ferrocene, the efg tensor is axially symmetric about the normal to the cyclopentadienyl rings,[20] and other studies[21,22] have shown that both V_{zz} and the isomer shift were quite insensitive to substitutions on the rings.

One can therefore conclude that the efg is also axially symmetric for the ferrocene derivatives.

The carbon–carbon bond linking the substituted tail to one of the π-cyclopentadienyl rings is coplanar with the ring. Therefore, the angle between the V_{zz} direction and this bond is $\pi/2$. If the tail were extended then the angle β between the long molecular axis as defined by the tail direction and V_{zz} would also be $\pi/2$. However, because the tail is "flexible" it is quite likely that there is a distribution of angles (β) between the effective tail direction and V_{zz} which is approximately symmetric about $\beta = \pi/2$. In the liquid crystalline glass, the distribution $f(\beta)$ will result from the "freezing in" of the smectic B distribution and be a function of steric packing considerations for the ferrocene derivative in the smectic B glass. Interestingly, the net effect of $f(\beta)$, if it is symmetric about $\pi/2$, will be similar to the effect of the liquid crystalline spatial distribution as per Eq. 1. That is, whether the long molecular axes are distributed about the external field direction or if in fact there is a distribution of V_{zz} directions about the normal to the long molecular axis, the effects on the π and σ transition probabilities will be similar. Both distributions tend to reduce the total range of A_π/A_σ values as θ varies from 0° to 90°. To introduce a symmetric distribution, $f(\beta)$, about $\beta = \pi/2$, in addition to the spatial distribution of the long axes about the magnetic field direction (Eq. 1) would not be useful here because they could not be experimentally separated. As a result, we will choose $f(\beta) = \delta(\cos\beta)$ and note that an S-value determined from a fit of Eq. 8 to the A_π/A_σ vs. θ data is really a lower limit on the solute order parameter for these ferrocene derivatives.

With $\beta = \pi/2$, the expression for $\cos\gamma$ (Eq. 6) simplifies:

$$\left(\beta = \frac{\pi}{2}\right)\cos\gamma = (\sin\psi\sin\delta\cos\theta - \cos\psi\sin\varepsilon\sin\theta - \cos\delta\cos\varepsilon\sin\psi\sin\theta) \tag{10}$$

Furthermore, since the glassy phase of BBOA is an ordinary smectic B phase, $\tau = 0$ and Eq. 3 becomes:

$$f_L \propto e^{\varepsilon_L \sin^2\theta} \tag{11}$$

From the area ratio data ε_M is known to be small so that $\exp(-\varepsilon_M\cos^2\gamma)$ can be expanded to first order in Eq. 7. The integrations are easily done and the recoil intensity ($f = f_L f_M$) normalized to the $\theta = 0°$ value becomes:

$$\frac{f(\theta)}{f(\theta=0)} = \frac{6 + \varepsilon_M[(3\cos^2\theta - 1)S - 2]}{6 + 2\varepsilon_M(S-1)}\, e^{\varepsilon_L \sin^2\theta} \tag{12}$$

where S is given by Eq. 9. A constant (C) is added to the right side of Eq. 12 in the fitting routine because it allows the entire theoretical curve to be

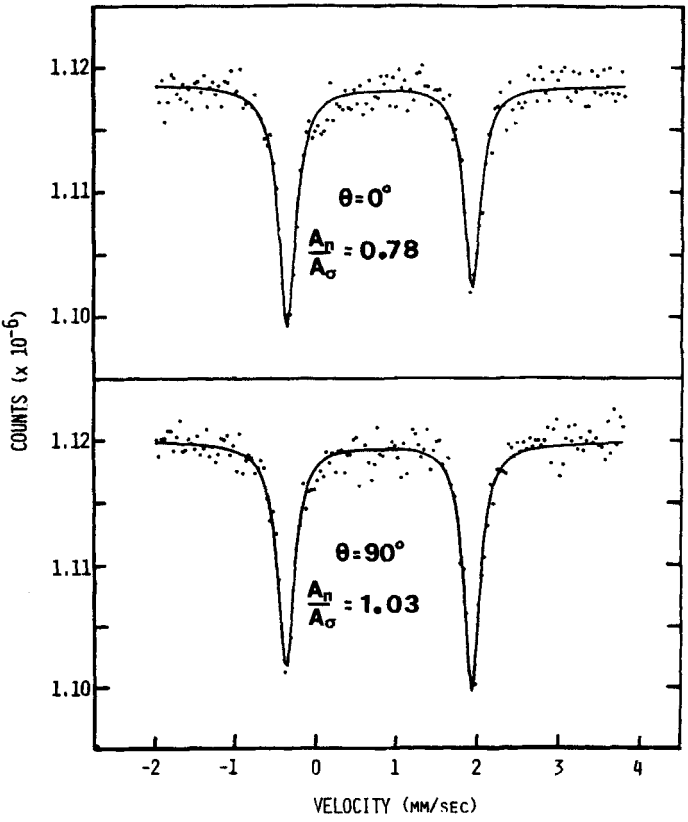

FIGURE 3 Mossbauer spectra for 0° and 90° alignment of FMA in BBOA. Both spectra are taken in the smectic B glass of BBOA (77 K). The solid lines are best fits of Lorentzian lineshapes to the experimental points.

raised or lowered without distorting its shape and has the effect of not forcing the theory and experiment to always coincide at $\theta = 0°$.[10]

Before Eq. 12 can be used to fit the f vs. θ data one must obtain the values for S and ε_M from fits of Eq. 8 to the A_π/A_σ vs. θ data. Starting with the condition that the orientational order parameter S must be greater than or equal to zero (indicating that if some preferential alignment exists it corresponds to alignment of the long molecular axes of the solutes parallel rather than perpendicular to the BBOA preferred molecular direction then the A_π/A_σ vs. θ data could only be fit with Eq. 8 if $V_{zz} > 0$ for each solute. This agrees with the data of Collins for ferrocene, itself.[20] Figures 4 and 5 are the best fits of Eqs. 8 [with $f(\beta) = \delta(\cos \beta)$] and 12, respectively, to the experimental data, while Table II lists the parameters that gave these fits. The area ratio gave

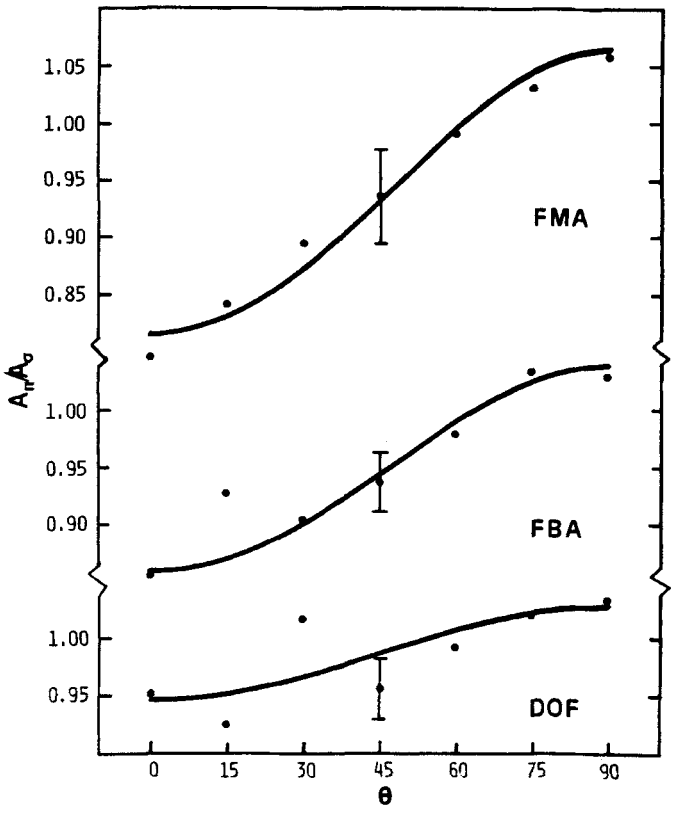

FIGURE 4 Plots of the area ratio (A_π/A_σ) vs. θ for the solutions of FMA, FBA, and DOF in BBOA. The data were all recorded at 77°K in the smectic B glass of BBOA.

q/kT and ε_M; the former parameter was used in Eq. 9 to evaluate S for each solute. These values of ε_M and S were then used as constants in fitting Eq. 12 to the f measurements to obtain ε_L and C.

Significantly, the two similar molecules FBA and FMA each gave $\varepsilon_M = 0.20$ indicating that the intramolecular vibrational amplitude parallel to $V_{zz}(\langle x_\parallel^2 \rangle_M)$ is greater than that normal to it ($\langle x^2 \rangle_M$). Conversely, $\varepsilon_M \approx 0$ for DOF implying that the intramolecular vibration is isotropic.

To within experimental error we have verified the above ε_M values by dissolving DOF, FBA, and FMA in butyl phthalate. Using approximately 1% molar solutions we have computed each ε_M from the A_π/A_σ data in the butyl phthalate glass at 77°K.[23] Ruby *et. al.*, have discussed the glass forming properties of butyl phthalate and determined $\varepsilon_M = -0.25$ for ferrocene at 77°K.[24] We have determined $\varepsilon_M = -0.30 \pm 0.10$ for ferrocene in butyl

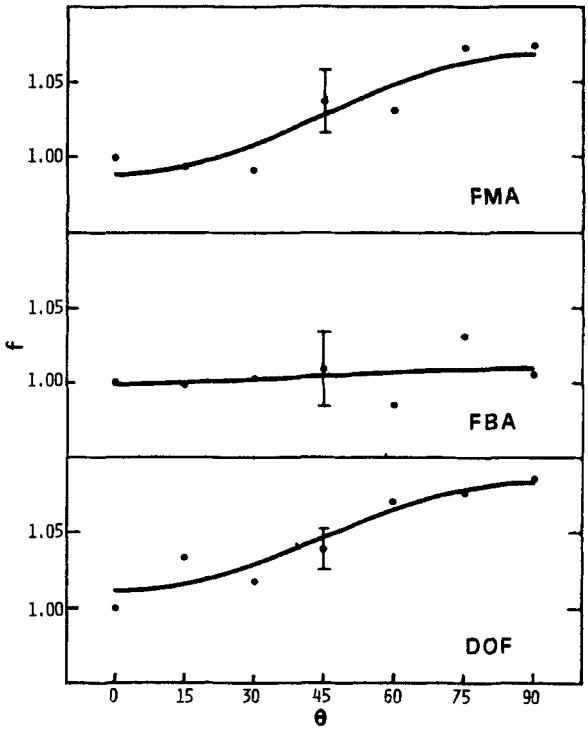

FIGURE 5 Plots of the Mossbauer intensity (f) vs. θ for the solutions of FMA, FBA, and DOF in BBOA. The data were all recorded at 77°K in the smectic B glass of BBOA.

phthalate in agreement with their data. Further, using the isotropic glass we find the following ε_M values: 0.21 ± 0.10 for FBA, 0.12 ± 0.10 for FMA, and 0.07 ± 0.10 for DOF. The verification of the liquid crystal data is clearly encouraging and gives one confidence in using the approximation that $f = f_L f_M$ and in choosing $f(\beta) = \delta(\cos \beta)$.

These results can be interpreted by considering the temperature dependence of f for ferrocene and its derivatives. Wertheim and Herber[21] first carried out such a study and Table III compares their result for ferrocene with those of the four ferrocene derivatives used in this study. In the 77°K to 298°K range the data show that relative to ferrocene, f decreases less rapidly on heating for disubstituted ferrocenes and more rapidly for monosubstituted ferrocenes.[21,22]

For molecular crystals in which the essential vibrational properties of the molecule are preserved in the solid, it is known that optical modes can significantly influence the recoil-free fraction. Infrared and Raman spectra showed that the only optical mode in ferrocene below room temperature is

TABLE II

Mossbauer parameters from best fits of Eqs. 8[a] and 17 to the experimental data

Compounds	S[b]	q/kT	ε_L[c]	ε_M[d]	C
1.5/2% DOF	0.11 ± .04	0.80	0.07 ± .02	0.00 ± .10	0.0119
1% FBA	0.27 ± .04	1.80	0.04 ± .02	0.20 ± .05	−0.0006
1% FMA	0.37 ± .06	2.50	0.12 ± .02	0.20 ± .05	−0.0108

[a] Here $f(\beta) = \delta(\cos\beta)$ was assumed.

[b] The main effect of the vibrational anisotropy ε_M is to either raise or lower the entire area ratio versus θ curve; what essentially determines the range R of A_π/A_σ values is the degree of alignment S of the molecules. In particular, if one assumes that $\varepsilon_M = 0$, $\tau = 0°$ (no tilt) and $f(\beta) = \delta(\cos\beta)$ then Eq. 8 becomes:

$$\frac{A_\pi}{A_\sigma}(\theta) = \frac{8 - (3\cos^2\theta - 1)S}{8 + (3\cos^2\theta - 1)S}$$

The range becomes

$$R = \frac{A_\pi}{A_\sigma}(90) - \frac{A_\pi}{A_\sigma}(0) = \frac{8 + S}{8 - S} - \frac{4 - S}{4 + S}$$

Using $R_{\min} = R_{\text{actual}} - 2\sigma_A$ and $R_{\max} = R_{\text{actual}} + 2\sigma_A$ (σ_A is the standard deviation for the experimental area ratio data) then one can obtain approximate values for $S_{\max}$ and $S_{\min}$. The resulting estimated error in S is given by $\Delta S = \pm(S_{\max} - S_{\min})/2$.

[c] The contribution of ε_M to the range of the f vs. θ dependence is very small compared to the ε_L contribution. As a result, by allowing $\varepsilon_M = 0$ and assuming that $\tau = 0°$, one finds that $f = f_L$ and Eq. 3 becomes:

$$\frac{f(\theta)}{f(\theta = 0)} = e^{\varepsilon_L \sin^2\theta}$$

Using the standard deviations (σ_f) in the f vs θ data in a manner similar to the above for the A_π/A_σ data, one can estimate an error in ε_L by

$$\Delta\varepsilon_L = \pm \frac{[\varepsilon_L(\max) - \varepsilon_L(\min)]}{2}.$$

[d] The error in the molecular contribution to the vibration anisotropy ($\Delta\varepsilon_M$) could not be obtained directly. If $\varepsilon_M = 0$, however, we see that $A_\pi/A_\sigma = 1$ for $\theta \approx 55°$ (see above). Therefore, as ε_M increases from zero the θ for which $A_\pi/A_\sigma = 1$ will change to $\theta \gtrless 55°$. As a result, the quality of the A_π/A_σ vs. θ data (insofar as it determines the θ for which $A_\pi/A_\sigma = 1$) can be used as rough gauge of ε_M. Clearly the data scatter for DOF is greater than for FMA and FBA (see Figure 4) and the estimates of $\Delta\varepsilon_M$ reflect this fact.

the ring-metal-ring symmetric bend at 170 cm^{-1} (245°K).[25] The next higher mode is at 478 cm^{-1} (689°K). Wertheim and Herber found that the iron recoil-free fraction declined more rapidly in the temperature range 77°–300°K for ferrocene than for both biferrocenyl and diferrocenyl mercury. This fact suggests that the lowest optical mode is shifted to a higher energy for bridged or substituted ferrocenes and therefore contributes less to the decline of f

TABLE III

Temperature dependence of the recoil-free fraction for ferrocene and its derivatives.

Compounds	Temperature (°K)	$f(T)/f(77°K)$
DOF[b]	298	0.36
	77	1.00
DFD[b]	298	0.32
	77	1.00
Ferrocene[a]	298	0.24
	77	1.00
FMA[b]	298	0.19
	77	1.00
FBA[b]	298	0.14
	77	1.00

[a] Ref. 21
[b] This work.

as the temperature increases. Stukan *et. al.*,[22] found that f decreased less rapidly with increasing temperature for disubstituted ferrocene derivatives than for ferrocene itself. This less rapid decline in f is due not only to the shift in the optical mode (245°K) to a higher energy because of the increased masses associated with the rings, but also due to the enhancement of intermolecular forces. An example of the latter is hydrogen bonding between O, Cl, and N containing substituents and the cyclopentadienyl rings. The increase in intermolecular forces is also operative for monosubstituted derivatives. However, Stukan *et al.*,[22] observed that relative to ferrocene the monosubstituted derivatives exhibit a greater decline of f as the temperature increases from 77°-300°K. They reasoned that in spite of the enhanced intermolecular bonding due to the single tail-ring interaction, the poorer packing caused by steric hindrance introduces new intramolecular optical modes which are effective in reducing f.

Table III compares the ratio $f(298°K)/f(77°K)$ for the four ferrocene derivatives discussed here with that of ferrocene itself. The two monosubstituted derivatives yield ratios lower than for ferrocene and the two disubstituted derivatives yield higher ones as expected. For the solutions of DOF, FMA and FBA in the BBOA glass the strengthening of the intermolecular forces due to interactions of the substituents with BBOA molecules should be similar to the pure compounds. Furthermore, the intramolecular modes for the individual molecules should be similar to the pure compounds.

Thus, the intramolecular vibrational modes will be more of a factor in determining f for the monosubstituted FBA and FMA than in determining f for the disubstituted DOF. In addition, the presence of additional intramolecular vibrational modes in the monosubstituted derivatives suggest that the vibrational anisotropy in these derivatives will be different from the anisotropy in the disubstituted derivatives or in ferrocene, itself. Assuming that the mass of the tail only increases the mass of the ring enables one to use the efg axis normal to the rings as a symmetry axis. This approximation will only be workable if, in fact, the measured values of ε_M are small indicating that the intramolecular motion of the Fe-atom is not only nearly axial but also nearly isotropic.

The agreement of the measured ε_M values for DOF, FMA, and FBA in the liquid crystalline glass and the isotropic glass is good. For the latter, the V_{zz} direction is necessarily assumed to be the axis of symmetry.[23] Therefore, the approximation that the V_{zz} axis is the axial intramolecular vibrational axis for the Fe-atoms in the liquid crystalline glass is internally consistent and reasonable. Further, since $\varepsilon_M > 0$ for FBA and FMA the vibrational amplitude parallel to the V_{zz} axis is enhanced relative to the vibrational amplitude normal to V_{zz} in the monosubstituted derivatives. That $\varepsilon_M \simeq 0.2$ for both FBA and FMA is also consistent with the fact that their tails are of roughly the same mass.

The small value of the order parameter ($S = 0.11$) for DOF implies that it possesses poor alignment in BBOA. This may be due to the two long octanoyl end-chains substituted on the ferrocene rings. Unlike the other two solutes (FMA and FBA), the DOF end-chains have no benzene rings. Therefore the attraction between the polarizable benzene ring and the polarizable central core region of BBOA molecules which helps align the end chains of FBA and FMA is not possible for DOF in BBOA. As a result, the DOF end chains are probably very disordered—possibly curling back on themselves or penetrating two adjacent layers and intertwining with several BBOA end-chains while the ferrocenyl bulk sits in between the smectic planes (end-chain region of the BBOA molecules). 1% FBA and 1% FMA have higher S values, 0.27 and 0.37, respectively. The ferrocene "head" is likely positioned in the end-chain region of the BBOA molecules, while the tail aligns in the direction of the BBOA long molecular axes in the central core region for the reason stated above. The higher degree of order for FMA may be due to the electric dipole moment of the methoxy group attached to its benzene ring. This dipole is parallel to the long molecular axis of the FMA molecule and may interact with a similar dipole of the butoxy group attached to the BBOA molecules to enhance order.

Equation 8 with $f(\beta) = \delta(\cos \beta)$ is not strictly applicable to the suspension of DFD (1%) in BBOA. If, however, one uses it to fit the A_π/A_σ data for

DFD, one can get a rough estimate of S for the microcrystallites. In this case, $S = 0.74$ for the DFD suspension. The large S value is consistent with the idea that relatively large crystallites would be more readily aligned by the liquid crystal molecules.[26]

The measured values of ε_L for FBA (0.04), DOF (0.07), and FMA (0.12) are small. The small lattice contribution to the vibrational anisotropy is consistent with the positioning of the bulky ferrocene group in the end-chain region of the BBOA layered structure. In particular, the end-chain region of the liquid crystalline molecules is known to be less ordered than the central-core regions and therefore less characteristic of the layer anisotropy.[27-30] The small ε_L values for the ferrocene derivatives are also consistent with the small ε_L value ($\varepsilon_L = -0.17$) found for the solute, tintetrabutyl (Sn–TB), in BBOA.[10] Both the ferrocene portion of the solutes of this paper and Sn–TB are bulky and approximately spherical in shape and would more likely find interstitial positions in the flexible tail region than the central-core region between the BBOA molecules. The difference in sign of ε_L for the iron solutes as compared to ε_L for Sn–TB probably lies in the local distortions of the BBOA tails in each individual case. The diameter of the Sn–TB (~ 12 Å) is about double that of $Fe(C_5H_5)_2$ (~ 6 Å). This, together with the fact that in FBA, FMA, and DOF the ferrocene group is attached to more or less aligned tails ($S > 0$ for each), must affect the positioning and distortion of the tails of the neighboring BBOA molecules.

V CONCLUSION

The area ratio data show that the BBOA molecules order the solute molecules (or small microcrystallites) of the ferrocene derivatives, and that V_{zz} is approximately perpendicular to their long molecular axes which align in the preferred direction of the BBOA molecules. This work confirms a positive electric field gradient tensor for ferrocene and its derivatives, and shows that the intramolecular vibrational anisotropy is greater for monosubstituted ferrocene derivatives than for disubstituted ferrocene derivatives which tend to have $\varepsilon_M = 0$. Confirmation of the above was obtained from temperature dependent intensity data on the ferrocene compounds which establishes greater importance of optical modes at 77°K for the monosubstituted derivatives FBA and FMA than for the disubstituted derivatives DOF and DFD.

The orientational order of the iron bearing impurities depends strongly on whether the impurity is present as a solute or a suspension of microcrystallites. Furthermore, the solute order parameter is greater for the monosubstituted ferrocene derivatives (FMA and FBA) which contain benzene

rings in the derivative tails than for the disubstituted derivative (DOF) which does not. The angular dependence of the Mossbauer intensity was found to be rather small for the three solutes. This resulted in rather low values for the lattice contribution to the nuclear vibrational anisotropy ε_L for each solute. The low ε_L values appear to establish the position of the ferrocene "head" of the solutes in the end-chain region of the host BBOA molecules.

Acknowledgement

The authors would like to thank Jack Stanford and Walter LaPrice for making the Mossbauer measurements in the butylphthalate solutions.

References

1. D. L. Uhrich, J. M. Wilson, and W. A. Resch, *Phys. Rev. Lett.*, **24**, 355 (1970).
2. J. M. Wilson and D. L. Uhrich, *Mol. Cryst.* and *Liq. Cryst.*, **13**, 85 (1971).
3. D. L. Uhrich, Y. Y. Hsu, D. L. Fishel, and J. M. Wilson, *Mol. Cryst.* and *Liq. Cryst.*, **20**, 349 (1973).
4. D. L. Uhrich, R. E. Detjen, and J. M. Wilson, in *Mossbauer Effect Methodology*, Vol. 8, edited by I. J. Gruverman and C. W. Seidel (Plenum, New York, 1973), p. 175.
5. R. E. Detjen, D. L. Uhrich, and C. F. Sheley, *Phys. Lett.*, **42A**, 522 (1973).
6. J. M. Wilson and D. L. Uhrich, *Mol. Cryst. and Liq. Cryst.*, **25**, 113 (1974).
7. D. L. Uhrich, J. Stroh, R. D'Sidocky, and D. L. Fishel, *Chem. Phys. Lett.*, **24**, 539 (1974).
8. V. I. Goldanskii, O. P. Kevdin, N. K. Kivrina, V. Y. Rochev, R. A. Stukan, I. T. Chistyakov, and L. S. Schabischev, *Mol. Cryst.* and *Liq. Cryst.*, **24**, 239 (1973).
9. M. J. Potasek, *Ph.D. Dissertation*, University of Illinois at Urbana-Champaign, 1974 (unpublished); M. J. Potasek, P. G. Debrunner, and G. DePasquali, *Phys. Rev.*, **A13**, 1605 (1976).
10. D. L. Uhrich, V. O. Aimiuwu, P. I. Ktorides, and W. J. LaPrice, *Phys. Rev.*, **12A**, 211 (1975).
11. G. H. Brown and W. G. Shaw, *Chem. Rev.*, **57**, 1049 (1957).
12. A. Saupe, *Angewand. Chem.*, **7**, 97 (1968).
13. V. O. Aimiuwu, *Ph.D. Dissertation*, Kent State University, 1976 (unpublished).
14. H. Goldstein, *Classical Mechanics*, (Addison-Wesley, Reading, Mass., 1965) p. 107.
15. V. I. Goldanskii and R. H. Herber, *Chemical Applications of Mossbauer Spectroscopy*, (Academic Press, New York, 1968).
16. E. Kankeleit, in *Mossbauer Effect Methodology*, Vol. 1, edited by I. J. Gruverman (Plenum, New York, 1965), p. 47.
17. W. A. Resch, *Master's Thesis*, Kent State University, (unpublished) 1971.
18. The BBOA was prepared and recrystallized by D. L. Fishel and R. D'Sidocky, Chemistry Department and Liquid Crystal Institute, Kent State University, Kent, Ohio 44242.
19. A. deVries, *Journal of Physics (Paris)*, **35**, 139 (1974); *Chem.-Phys. Letters*, **28**, 252 (1974).
20. R. L. Collins, *J. Chem. Phys.*, **42**, 1072 (1965).
21. G. K. Wertheim and R. H. Herber, *J. Chem. Phys.*, **38**, 2106 (1963).
22. R. A. Stukan, S. P. Gubin, A. N. Nesmeyanov, V. I. Goldanskii, and E. F. Makarov, *Teor. i eKsp. Khim.*, **2**, 805 (1966); *Theor. Exp. Chem. (USSR)*, **2**, 581 (1966).
23. P. A. Flinn, S. L. Ruby, and W. Z. Kehl, *Science*, **143**, 1434 (1964).
24. S. L. Ruby, B. J. Zabransky, and P. A. Flinn, *J. de Physique* (to be published); and P. A. Flinn, private communication.
25. E. R. Lippincott and R. D. Nelson, *Spectrochimica Acta*, **10**, 307 (1958).
26. If one applies the model of the present paper to the data for the suspension of 1,1'-diacetylferrocene crystallites in 4-4'-bis(heptyloxy)azoxybenzene (reference 6) the resulting order parameter is $S \approx 1.0$. This result is consistent with the results of the present paper.

27. J. A. Murphy, J. W. Doane, and D. L. Fishel, in *Symposium on Ordered Fluids and Liquid Crystals*, (American Chemical Society, Chicago, 1973).
28. W. L. McMillan, *Phys. Rev.*, **A4**, 1238 (1971).
29. S. Marčelja, *Solid State Commun.*, **13**, 759 (1973).
30. M. Dvolaitsky, F. Poldy, and L. Taupin, *Phys. Lett.*, **45A**, 454 (1973).